JOC*Article*

The Reaction of Cyclopentyne with Ethene: Concerted vs Stepwise Mechanism?

Steven M. Bachrach*,† and John C. Gilbert*,‡

Department of Chemistry, Trinity University, 1 Trinity Place, San Antonio, Texas 78212, and Department of Chemistry and Biochemistry, The University of Texas at Austin, 1 University Station, Austin, Texas 78712

sbachrach@trinity.edu

Received April 27, 2004

The cycloaddition of cyclopentyne with ethene was examined using (U)B3LYP and CASSCF methods to discern the reaction mechanism. (U)B3LYP/6-31G* and (U)B3LYP/6-311+G* slightly favor the concerted pathway, whereas CASSCF(4,4)/6-31G* and CASCF(6,6)/6-31G* favor the diradical pathway. MRMP2 using the CASSCF(4,4) wave function also favors the diradical mechanism. In the context of a diradical pathway, the experimentally observed complete retention of stereochemistry for this reaction is understood in terms of stereochemical control resulting from dynamic effects.

The cycloaddition chemistry of cyclopentyne (**1**) has intrigued chemists since the discovery of its reactions with alkenes in 1983.[1] A [2 + 2] cycloadduct is formed in the reaction, remarkably with complete retention of stereochemistry, as indicated in Scheme 1.[2,3] As understood within the framework of orbital symmetry arguments, symmetry conservation of this type is formally forbidden by the Woodward−Hoffmann rules.[4] While some tentative arguments had been put forth to explain this "violation" of the rules, by proposing involvement of either an anti-symmetric diradical[3] or a lumomer,[5] we recently reported experimental[6] and theoretical[7] evidence for an alternative reaction mechanism that is consistent with the tenets of orbital symmetry.

In the reaction of norbornyne (**2**) with 2,3-dihydropyran, Laird and Gilbert[6] observed the expected [2 + 2] adduct **3**, along with the polycyclic adduct **4**. They proposed the mechanism given in Scheme 2 to account for these products. Concurrently, we examined this mechanism theoretically using B3LYP/6-31G* computations.[7] A concerted [2 + 1] transition state was located connecting reactants (either cyclopentyne and ethene or norbornyne and ethene) with the cyclopropylcarbene intermediate. The free energy activation barrier is almost entirely entropic in nature, and the addition is strongly exoergonic. The cyclopropylcarbene can then undergo a 1,2-C shift with a small barrier to give the stereoretention product, consistent with the experimental observations.

SCHEME 1

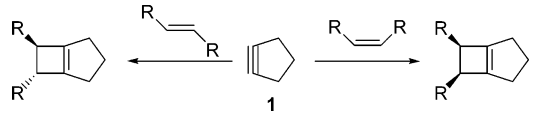

SCHEME 2

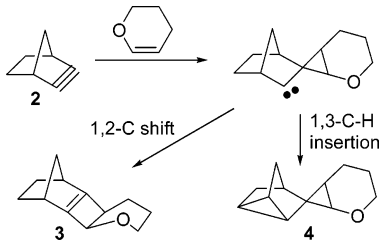

In this paper, we present further computational results concerning the mechanism for the reaction of cyclopentyne with ethene, specifically comparing this concerted [2 + 1] addition with a stepwise diradical mechanism.

Computational Methods

The two mechanisms under investigation here involve carbene and diradical(oid) species, both of which offer challenges for the computational chemist. Toward that end, we have completely optimized the structures involved in the reaction of cyclopentyne with ethene along a concerted and a stepwise pathway (see Scheme 3) using a number of computational techniques. The B3LYP/6-31G* and B3LYP/6-311+G** models were used for the concerted path, whereas the UB3LYP functional was used for the diradical path.[8] For an alternative treatment of correlation, we used CAS(4,4)/6-31G* and CAS(6,6)/6-31G*,[9] where the former uses an active space

† Trinity University.
‡ The University of Texas at Austin.

(1) Gilbert, J. C.; Baze, M. E. *J. Am. Chem. Soc.* **1983**, *105*, 664−665.
(2) Gilbert, J. C.; Baze, M. E. *J. Am. Chem. Soc.* **1984**, *106*, 1885−1886.
(3) Fitjer, L.; Modaressi, S. *Tetrahedron Lett.* **1983**, *24*, 5495−5498.
(4) Woodward, R. B.; Hoffmann, R. *Angew. Chem., Int. Ed. Engl.* **1969**, *8*, 781−853.
(5) (a) Gilbert, J. C.; Kirschner, S. *Tetrahedron Lett.* **1993**, *34*, 599−602. (b) Gilbert, J. C.; Kirschner, S. *Tetrahedron Lett.* **1993**, *34*, 603−606.
(6) Laird, D. W.; Gilbert, J. C. *J. Am. Chem. Soc.* **2001**, *123*, 6704−6705.
(7) Bachrach, S. M.; Gilbert, J. C.; Laird, D. W. *J. Am. Chem. Soc.* **2001**, *123*, 6706−6707.
(8) (a) Becke, A. D. *J. Chem. Phys.* **1993**, *98*, 5648−5650. (b) Lee, C.; Yang, W.; Parr, R. G. *Phys. Rev. B* **1988**, *37*, 785−789. (c) Vosko, S. H.; Wilk, L.; Nusair, M. *Can. J. Phys.* **1980**, *58*, 1200−1211. (d) Stephens, P. J.; Devlin, F. J.; Chabalowski, C. F.; Frisch, M. J. *J. Phys. Chem.* **1994**, *98*, 8, 11623−11627.

10.1021/jo0492970 CCC: $27.50 © 2004 American Chemical Society
Published on Web 08/24/2004

SCHEME 3

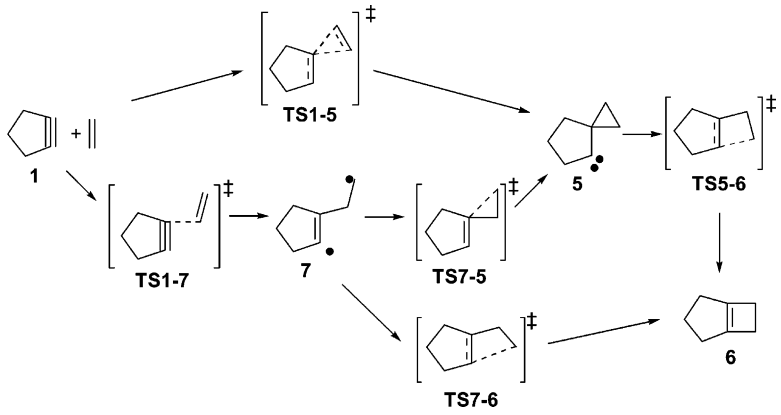

confined to only the direct bond making and breaking, while the latter active space also includes the second π-bond of the precursor cycloalkyne. To include dynamical correlation with the CAS wave function, we have computed the MRMP2/6-31G*//CASSCF(4,4)/6-31G* energies for some structures.[10]

Analytical frequencies were computed for all structures to confirm the nature of each critical point, and zero-point vibrational energies (ZPE) and free energies were obtained as well. All frequencies and ZPEs were used without scaling. Free energies were computed at 298 K using standard partition-function approximations.[11] All computations were performed using either GAUSSIAN-98[12] or GAUSSIAN-03,[13] except the MRMP2 computations, which were done with GAMESS.[14]

Results

Invoking the mechanism of Laird and Gilbert,[6] the reaction of cyclopentyne with ethene should first create the cyclopropylcarbene intermediate **5**. The carbene then undergoes a 1,2-C shift, passing through the transition state **TS5**−**6**, to give bicyclo[3.2.0]hept-1(5)-ene (**6**). Our principal focus for this work is on the first stage of this process, namely how do cyclopentyne and ethene combine to give **5**? In our previous study, we examined only the concerted [2 + 1] cycloaddition where **TS1**−**5** is the sole transition structure for this conversion. We now examine the possibility of a stepwise, nonconcerted mechanism whereby cyclopentyne and ethene first combine to form the diradical intermediate **7**, passing through transition state **TS1**−**7**. A second chemical step closes the three-member ring, passing through **TS7**−**5**, to produce cyclopropylcarbene **5**.

The Concerted Path 1 → 5. In Table 1, we present some of the geometric parameters for **1** and **5** and the transition state connecting them. The B3LYP/6-31G* geometries are also drawn in Figure 1. We have not optimized cyclopentyne at CASSCF(6,6) because there is no need to correlate the σ-bonding electrons, especially in comparison with the rest of the reaction pathway. The structure of cyclopentyne (**1**) is little affected by the computational method. The triple bond is a little longer (about 0.03 Å) at CASSCF than with B3LYP, suggesting that the latter method may not account properly for diradical character in **1**. Similarly, the computational method has little effect on the structure of the cyclopropylcarbene **5**. The only difference is that the C_1-C_2 bond is about 0.03 Å shorter at B3LYP than at CASSCF.

There is some question as to the lowest energy spin state of **5**. We have optimized the structure of its triplet spin state at B3LYP/6-31G*, and its geometry is reported in Table 1. As expected,[15,16] the angle about the carbenic center is wider in the triplet than in the singlet: 103.03° vs 115.38°. The $C_1-C_2-C_3$ angle is concomitantly smaller in the triplet. The C−C distances in the three-membered ring are shorter in the triplet than the singlet, though C_1-C_2 is longer in the former species. Most importantly, the singlet state is 12.3 kcal mol^{-1} lower in energy than the triplet. Given that recent studies have shown that B3LYP/6-31G* overestimates the stability of the triplet relative to the singlet of a variety of small carbenes by a few kcal mol,[1,17−20] we can safely conclude that the singlet state of **5** is the ground state.

(9) (a) Hegarty, D.; Robb, M. A. *Mol. Phys.* **1979**, *38*, 1795−1812. (b) Eade, R. H. A.; Robb, M. A. *Chem. Phys. Lett.* **1981**, *83*, 362−368. (c) Yamamoto, N.; Vreven, T.; Robb, M. A.; Frisch, M. J.; Schlegel, H. B. *Chem. Phys. Lett.* **1996**, *250*, 373−378.

(10) Hirao, K. *Chem. Phys. Lett.* **1992**, *190*, 374−380.

(11) Cramer, C. J. *Essentials of Computational Chemistry. Theories and Models*; John Wiley: Chichester, U.K., 2002.

(12) Frisch, M. J.; Trucks, G. W.; Schlegel, H. B.; Scuseria, G. E.; Robb, M. A.; Cheeseman, J. R.; Zakrzewski, V. G.; Montgomery, J. A. J.; Stratmann, R. E.; Burant, J. C.; Dapprich, S.; Millam, J. M.; Daniels, A. D.; Kudin, K. N.; Strain, M. C.; Farkas, O.; Tomasi, J.; Barone, V.; Cossi, M.; Cammi, R.; Mennucci, B.; Pomelli, C.; Adamo, C.; Clifford, S.; Ochterski, J.; Petersson, G. A.; Ayala, P. Y.; Cui, Q.; Morokuma, K.; Malick, D. K.; Rabuck, A. D.; Raghavachari, K.; Foresman, J. B.; Cioslowski, J.; Ortiz, J. V.; Baboul, A. G.; Stefanov, B. B.; Liu, G.; Liashenko, A.; Piskorz, P.; Komaromi, I.; Gomperts, R.; Martin, R. L.; Fox, D. J.; Keith, T.; Al-Laham, M. A.; Peng, C. Y.; Nanayakkara, A.; Gonzalez, C.; Challacombe, M.; Gill, P. M. W.; Johnson, B.; Chen, W.; Wong, M. W.; Andres, J. L.; Gonzalez, C.; Head-Gordon, M.; Replogle, E. S.; Pople, J. A. Gaussian, Inc.: Pittsburgh, PA, 1998.

(13) Frisch, M. J.; Trucks, G. W.; Schlegel, H. B.; Scuseria, G. E.; Robb, M. A.; Cheeseman, J. R.; Montgomery, J., J. A.; Vreven, T.; Kudin, K. N.; Burant, J. C.; Millam, J. M.; Iyengar, S. S.; Tomasi, J.; Barone, V.; Mennucci, B.; Cossi, M.; Scalmani, G.; Rega, N.; Petersson, G. A.; Nakatsuji, H.; Hada, M.; Ehara, M.; Toyota, K.; Fukuda, R.; Hasegawa, J.; Ishida, M.; Nakajima, T.; Honda, Y.; Kitao, O.; Nakai, H.; Klene, M.; Li, X.; Knox, J. E.; Hratchian, H. P.; Cross, J. B.; Adamo, C.; Jaramillo, J.; Gomperts, R.; Stratmann, R. E.; Yazyev, O.; Austin, A. J.; Cammi, R.; Pomelli, C.; Ochterski, J. W.; Ayala, P. Y.; Morokuma, K.; Voth, G. A.; Salvador, J.; Dannenberg, J. J.; Zakrzewski, V. G.; Dapprich, S.; Daniels, A. D.; Strain, M. C.; Farkas, O.; Malick, D. K.; Rabuck, A. D.; Raghavachari, K.; Foresman, J. B.; Ortiz, J. V.; Cui, Q.; Baboul, A. G.; Clifford, S.; Cioslowski, J.; Stefanov, B. B.; Liu, G.; Liashenko, A.; Piskorz, P.; Komaromi, I.; Martin, R. L.; Fox, D. J.; Keith, T.; Al-Laham, M. A.; C. Y. Peng, C. Y.; Nanayakkara, A.; Challacombe, M.; Gill, P. M. W.; Johnson, B.; Chen, W.; Wong, M. W.; Gonzalez, C.; Pople, J. A. Gaussian, Inc.: Pittsburgh, PA, 2003.

(14) Schmidt, M. W.; Baldridge, K. K.; Boatz, J. A.; Elbert, S. T.; Gordon, M. S.; Jensen, J. H.; Koseki, S.; Matsunaga, N.; Nguyen, K. A.; Su, S.; Windus, T. L.; Dupuis, M.; Montgomery, J. A. *J. Comput. Chem.* **1993**, *14*, 1347−1363.

(15) Harrison, J. F. *Acc. Chem. Res.* **1974**, *7*, 378−384.

(16) Trozzolo, A.; Wasserman, E. In *Carbenes*; Moss, R. A., Jones, M., Eds.; J. Wiley: New York, 1975; Vol. II, pp 185−206.

TABLE 1. Optimized Geometrical Parameters for Cyclopentyne 1, TS1-5 and 5 (all Distances Are in Å and all Angles Are in deg)

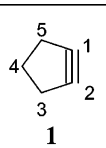

1

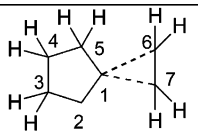

TS1-5

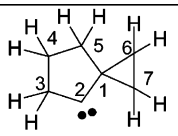

5

1							
	C_1-C_2	C_2-C_3	C_3-C_4	C_5-C_1-C_2	C_2-C_3-C_4		
B3LYP/6-31G*	1.226	1.509	1.590	115.87	98.82		
B3LYP/6-311+G**	1.220	1.509	1.590	116.04	98.73		
CAS(4,4)/6-31G*	1.250	1.508	1.571	114.87	99.68		
TS1-5							
	C_1-C_2	C_1-C_6	C_1-C_7	C_6-C_7	C_6-C_1-C_7	C_2-C_1-C_5	C_1-C_2-C_3
B3LYP/6-31G*	1.263	2.504	2.534	1.343	30.91	134.07	96.26
B3LYP/6-311+G**	1.258	2.444	2.465	1.342	31.72	131.79	98.27
CAS(4,4)/6-31G*	1.292	2.079	2.086	1.346	37.71	126.13	100.42
CAS(6,6)/6-31G*	NF[a]						
5							
	C_1-C_2	C_1-C_6	C_1-C_7	C_6-C_7	C_6-C_1-C_7	C_2-C_1-C_5	C_1-C_2-C_3
B3LYP/6-31G* S[b]	1.447	1.577	1.522	1.478	56.94	113.99	103.02
B3LYP/6-31G* T[c]	1.464	1.531	1.516	1.504	59.13	103.07	115.38
B3LYP/6-311+G**	1.439	1.579	1.526	1.474	56.66	113.50	103.90
CAS(4,4)/6-31G*	1.468	1.566	1.506	1.478	57.46	112.55	103.03
CAS(6,6)/6-31G*	1.488	1.577	1.500	1.478	57.37	112.57	102.39

[a] Structure did not optimize at this level. [b] Singlet [c] Triplet

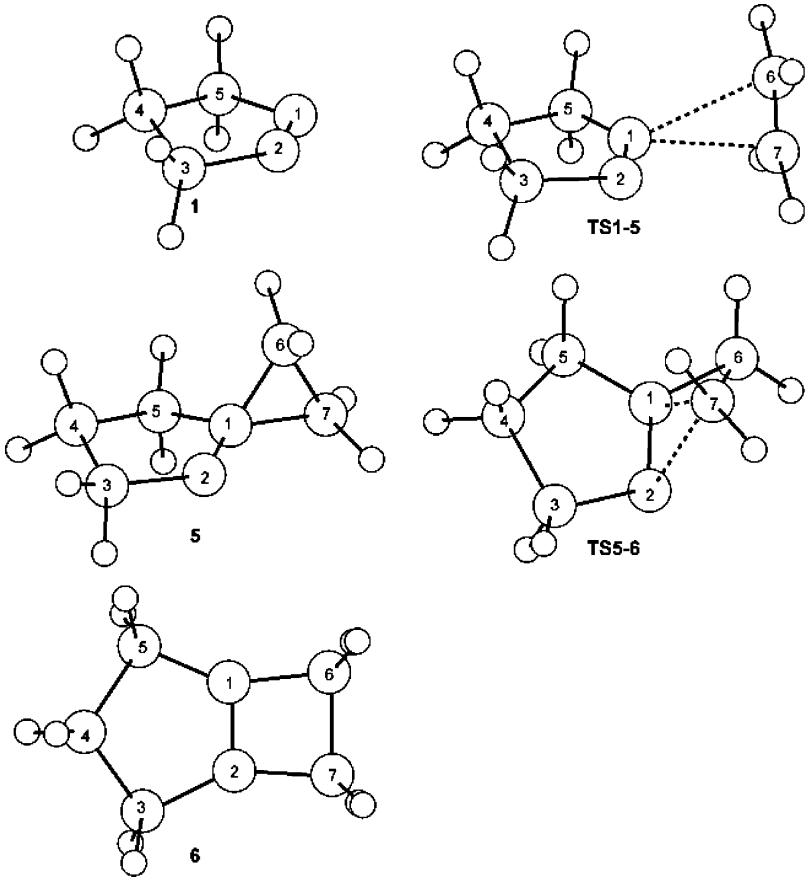

FIGURE 1. B3LYP/6-31G*-optimized geometries of the critical points along the concerted pathway.

TABLE 2. Relative Free Energies (kcal mol^{-1})

	TS1−5	TS1−7	7	TS7−5	5	TS5−6	TS7−6	6
(U)B3LYP/6-31G*[a]	36.47	37.14	9.08	19.81	0.0	5.70	10.94	−48.81
(U)B3LYP/6-311+G**[a]	33.78	NF[c]	9.80	19.77	0.0	6.28	11.61	−45.29
CAS(4,4)/6-31G*	43.25	34.58	−0.95	20.69	0.0	12.10	1.56	−32.95
MRMP2/6-31G*[b]	43.26	33.64	1.70	12.34	0.0			−53.90
CAS(6,6)/6-31G*	NF[d]	22.40	−4.71	27.91	0.0	8.89	12.55	−36.79

[a] UB3LYP was used for all structures with diradical character; otherwise, RB3LYP was employed. [b] MRMP2 electronic energy calculated from the CASSCF(4,4) wave function at the CASSCF(4,4)/6-31G*-optimized geometry. [d] All attempts to optimize this transition state led to dissociated reactants or **TS1−5**. [d] All attempts to optimize this transition state led to **TS1−7**.

TABLE 3. Optimized Geometrical Parameters for TS1-7, 7, and TS7-5 (all Distances Are in Å and all Angles Are in deg)

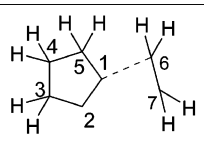

TS1-7

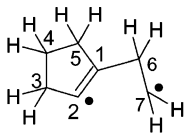

7

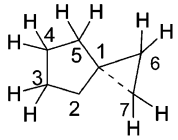

TS7-5

	C_1-C_2	C_1-C_6	C_1-C_7	C_6-C_7	C_1-C_6-C_7	C_2-C_1-C_5	C_1-C_2-C_3
TS1-7							
UB3LYP/6-31G*	1.259	2.315	2.979	1.353	105.62	117.36	112.03
UB3LYP/6-311+G**							
CAS(4,4)/6-31G*	1.257	2.149	2.898	1.379	108.42	113.72	115.17
CAS(6,6)/6-31G*	1.274	2.100	2.867	1.383	109.09	113.62	114.39
7							
UB3LYP/6-31G*	1.326	1.505	2.515	1.498	113.72	107.87	117.71
UB3LYP/6-311+G**	1.322	1.504	2.515	1.495	113.98	107.79	118.00
CAS(4,4)/6-31G*	1.333	1.513	2.533	1.504	114.19	108.54	116.01
CAS(6,6)/6-31G*	1.349	1.512	2.532	1.504	114.12	108.25	115.71
TS7-5							
UB3LYP/6-31G*	1.363	1.516	2.092	1.471	88.88	111.65	109.62
UB3LYP/6-311+G**	1.356	1.519	2.114	1.469	90.02	111.65	109.95
CAS(4,4)/6-31G*	1.386	1.502	2.086	1.475	88.96	112.74	106.09
CAS(6,6)/6-31G*	1.384	1.503	2.116	1.477	90.47	112.75	106.16

Unlike for **1** and **5** where the computational methods provide very similar structures, the geometry of the transition state connecting these two (**TS1−5**) is very dependent on methodology. The two B3LYP geometries are similar; the magnitude of the distances (2.4 to 2.5 Å) for the C−C bonds being formed and the fact that the C_6−C_7 distance is barely increased from that in ethene suggest a very early transition state. On the other hand, the CASSCF(4,4) transition state is later: the forming C−C bonds are now just slightly longer than 2 Å. Despite repeated efforts at locating a [2 + 1] transition state using CASSCF(6,6), the only transition state located is decidedly asymmetric with respect to the C_1−C_6 and C_1−C_7 distances and is in fact **TS1−7**, discussed below. These differences hint at the possibility of an alternate pathway.

To conclude the discussion of the concerted [2 + 1] path, we present in Table 2 the energies of **TS1−5** relative to the intermediate carbene **5**. Since the configuration spaces that might be used for the reactants are not identical in size to those for the intermediates and products, direct comparison of the energies of reactants with the other critical points is problematic. Therefore, we use **5** as the reference point. B3LYP/6-311+G** and B3LYP/6-31G* place the transition state about 34 and 36 kcal mol^{-1} above **5**. CASSCF(4,4) predicts a higher energy for this transition state, about 43 kcal mol^{-1}.

The Diradical Path 1 → 5. Cyclopentyne and ethene can react to produce the cyclopropylcarbene intermediate **5** via an alternative mechanism that involves the formation of a diradical intermediate. This diradical pathway is outlined in Scheme 3. Ethene and cyclopentyne can approach each other in an asymmetric way, passing through **TS1−7** to create the diradical **7**. This diradical can then close, progressing through **TS7−5**, to give **5**.

Important geometric parameters of the critical points along this diradical path are listed in Table 3, and the B3LYP/6-31G* structures are drawn in Figure 2. All four computational models give similar geometries of the diradical intermediate **7**. The C_1−C_2 distance is consistent with a typical double bond, and the C_6−C_7 distance is near that typical for a single bond.

Greater variation among the computational methods is found for the structure of **TS1−7**. CASSCF computations predict a slightly later transition state: the forming C_1−C_6 bond is about 0.2 Å shorter and the C_6−C_7 is some 0.03 Å longer with the CASSCF models than with the B3LYP models. Whether the internal ring angle at C_1 or C_2 is larger is also dependent on the method; CASSCF again indicates a later TS with a smaller angle at C_1 and

(17) Vargas, R.; Galvan, M.; Vela, A. *J. Phys. Chem. A* **1998**, *102*, 3134−3140.
(18) Hu *Chem. Phys. Lett.* **1999**, *309*, 81−89.
(19) Scott, A. P.; Platz, M. S.; Radom, L. *J. Am. Chem. Soc.* **2001**, *123*, 6069−6076.
(20) Das, D.; Whittenburg, S. L. *THEOCHEM* **1999**, *492*, 175−186.

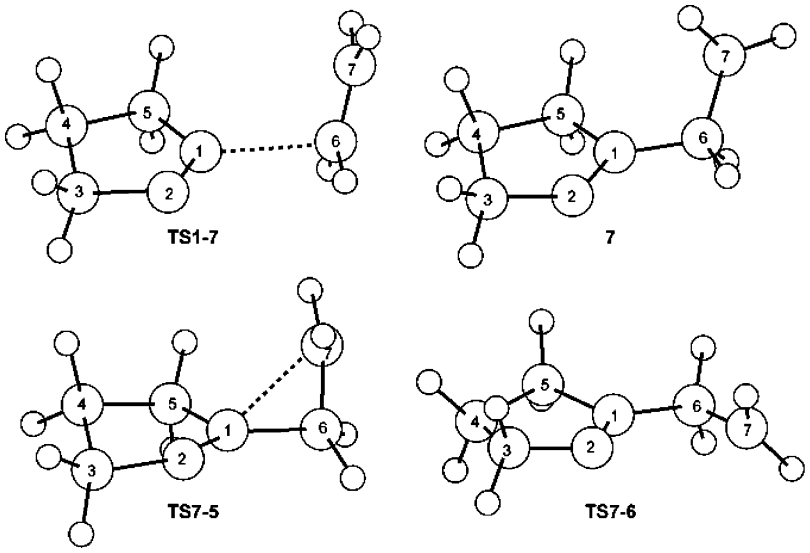

FIGURE 2. (U)B3LYP/6-31G*-optimized geometries of the critical points along the diradical pathway.

wider at C_2. Perhaps the more interesting result is that despite repeated attempts, we were unable to locate a transition state that corresponds to the **TS1-7** using UB3LYP/6-311+G**. All optimizations either led to dissociated reactants or to the concerted **TS1**−**5** structure previously obtained. In other words, the unrestricted wave function collapses to the restricted wave function and only the concerted TS exists on this surface. Hrovat, Duncan, and Borden reported a similar situation in their study of the Cope rearrangement of 1,2,6-heptatriene; attempts to locate a transition state at UB3LYP collapsed to the spin-restricted B3LYP-concerted path solution.[21]

The four computational models provide very similar geometries for **TS7**−**5**, the transition state connecting the diradical intermediate **7** with the cyclopropylcarbene **5**. The forming C_1-C_7 bond is about 2.1 Å and the $C_1-C_6-C_7$ angle is around 90°. The C_1-C_2 distance is 1.36 Å (B3LYP) or 1.38 Å (CASSSCF). These distances and angles indicate an early transition state, with much geometric change still needed to create **5**.

The relative energies of the critical points along the diradical pathway are listed in Table 2. These predicted energetics split along methodological lines. The major difference between the DFT and CASSCF potential energy surfaces is the relative energies of **5** and **7**. All four models do locate local minima that correspond to **5** and **7**. Both (U)B3LYP computations suggest that the diradical intermediate **7** lies 9−10 kcal mol^{-1} above the carbene **5**. There is significant spin contamination for the diradical **7** ($S^2 = 1.01$) and this is consistent with the unrestricted DFT representation of this state as a 50:50 mixture of the singlet and triplet states. The sum model[22] can be used to obtain the energy of the singlet as twice the energy of the 50:50 state, less the energy of the triplet. The triplet lies only 0.04 kcal mol^{-1} above the 50:50 state. Thus, the energy correction for the true singlet is essentially nil, leaving diradical **7** well above cyclopropylcarbene **5**. Along with the fact that singlet **5** is more stable than triplet **5**, this indicates that the cycloaddition will take place on the singlet surface. On the other hand, both CASSCF computations indicate the opposite, namely that **7** is more stable than **5**. CASSCF(4,4) predicts that **7** is only 1 kcal mol^{-1} below **5**, while the larger CASSCF(6,6) computation increases this difference to 4.7 kcal mol^{-1}. It is expected that DFT would favor a closed-shell structure over a diradical structure, since the DFT wave function is restricted to a single Slater determinant.[11] Previous studies of the Cope and Claisen rearrangements, which compare diradical vs concerted pathways, generally find a small difference like we see here.[21,23]

As indicated previously, we could not locate **TS1**−**7** at UB3LYP/6-311+G**. However, we were successful with the other models. At B3LYP/6-31G*, **TS1**−**7** is 28.08 kcal mol^{-1} higher in energy than **7**. This is quite similar to the CASSCF(6,6) result (27.11 kcal mol^{-1}), but CASSCF(4,4) predicts a higher barrier, viz., 35.53 kcal mol^{-1}.

The two DFT models give very similar energies for the closing of the diradical **7** to the cyclopropylcarbene **5**: 10.73 kcal mol^{-1} with the smaller basis set and 9.97 kcal mol^{-1} with the larger one. On the other hand, the two CASSCF calculations indicate a higher barrier and disagree on its value. The barrier is 21.64 kcal mol^{-1} at CASSCF(4,4) but 32.62 kcal mol^{-1} at CASSCF(6,6).

CASSCF tends to favor diradicals over closed-shell species. This artifact can be minimized by performing MP2 calculations from the CASSCF wave function. We computed the MRMP2 energies using the CASSCF(4,4) wave function at the CASSCF(4,4) optimized geometries. These relative electronic energies are listed in Table 2. The relative energies of the two transition states **TS1**−**5** and **TS1**−**7** are minimally affected by the inclusion of dynamic correlation; the transition state to the diradical intermediate is still favored by 10 kcal mol^{-1}. The MRMP2 calculations, however, reverse the relative stabilities of **5** and **7** from the CASSCF results; with

(21) Hrovat, D. A.; Duncan, J. A.; Borden, W. T. *J. Am. Chem. Soc.* **1999**, *121*, 161−175.

(22) (a) Ziegler, T.; Rauk, A.; Baerends, E. J. *Theor. Chim. Acta* **1977**, *43*, 261−271. (b) Cramer, C. J.; Dulles, F. J.; Giessen, D. J.; Almlof, J. *Chem. Phys. Lett.* **1995**, *245*, 165−170.

(23) Wiest, O.; Black, K. A.; Houk, K. N. *J. Am. Chem. Soc.* **1994**, *116*, 10336−10337.

TABLE 4. Optimized Geometrical Parameters for TS5-6, TS7-6, and 6 (all Distances Are in Å and all Angles Are in deg)

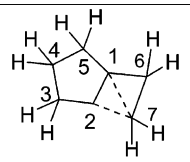

TS5-6

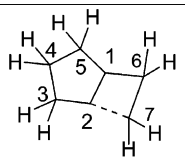

TS7-6

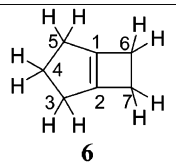

6

	C_1-C_2	C_1-C_6	C_2-C_7	C_6-C_7	C_1-C_6-C_7	C_2-C_1-C_5	C_1-C_2-C_3
TS5-6							
B3LYP/6-31G*	1.403	1.486	1.926	1.518	69.54	116.20	103.82
B3LYP/6-311+G**	1.397	1.485	1.930	1.518	70.21	115.77	104.67
CAS(4,4)/6-31G*	1.392	1.481	1.964	1.505	72.69	115.93	104.37
CAS(6,6)/6-31G*	1.418	1.480	1.984	1.502	72.06	115.78	103.42
TS7-6							
B3LYP/6-31G*	1.326	1.511	3.217	1.496	113.80	107.82	117.73
B3LYP/6-311+G**	1.321	1.508	3.221	1.493	114.24	107.73	118.10
CAS(4,4)/6-31G*	1.335	1.518	3.223	1.504	114.23	108.32	116.04
CAS(6,6)/6-31G*	1.334	1.504	3.217	1.519	114.21	108.33	116.03
6							
B3LYP/6-31G*	1.331	1.524	1.524	1.585	85.22	114.18	114.18
B3LYP/6-311+G**	1.328	1.525	1.525	1.586	85.16	114.23	114.23
CAS(4,4)/6-31G*	1.309	1.518	1.518	1.609	84.33	114.36	114.36
CAS(6,6)/6-31G*	1.326	1.518	1.518	1.613	84.58	113.95	113.95

inclusion of dynamic correlation the carbene intermediate is now slightly favored (by almost 2 kcal mol^{-1}) over the diradical intermediate.

The Concerted Path 5 → 6. The cycloproylcarbene **5** can undergo a concerted [1,2]-C migration, opening up the three-membered ring to form the final product **6**. Important geometrical parameters of the optimized structures of the transition state for this reaction (**TS5−6**) and **6** are listed in Table 4, and the B3LYP/6-31G* structures are drawn in Figure 1.

The four computational models predict quite comparable structures for **TS5−6**. The largest difference is that CASSCF predicts a longer C_2−C_7 distance than does DFT. All four models also give nearly identical structures for **6**. Here, the largest difference is in the C_6−C_7 distance, predicted to be about 0.02 Å longer with CAS than with DFT.

The predicted barrier from **5** ranges from 5.7 to 12.55 kcal mol^{-1}, with the DFT results on the lower end and CAS results on the higher end. The reaction is quite exergonic; DFT indicates ΔG is about −47 kcal mol^{-1}, while the CAS computations suggest a slightly lesser value of −34 kcal mol^{-1}.

The Diradical Path 7 → 6. If the reaction of cyclopentyne and ethene proceeds via the diradical intermediate **7**, then it is possible for the overall product **6** to be directly formed without creating **5**. We have located the transition state for this direct closure, which basically involves rotation about the exocyclic C−C bond to bring the two formal radical centers close to coplanar. Once the diradical centers are close, the ring forms without further barriers.

The UB3LYP/6-31G* structure of **TS7−6** is shown in Figure 2, and geometric parameters for all four models are listed in Table 4. The geometries are in excellent agreement with each other. On the other hand, although UB3LYP/6-31G*, UB3LYP/6-311+G** and CASSCF(4,4)/6-31G* all predict that **TS7−6** lies about 2 kcal mol^{-1} above **7**, the barrier is much higher at CASSCF(6,6)/6-31G*, 17.26 kcal mol^{-1}. While this disparity is disconcerting, the more important point is that the barrier for the path **7 → 6** is lower than the barrier for the competing path, **7 → 5**.

Discussion

Any proposed mechanism for the reaction of cyclopentyne with ethene must account for the observations of complete stereoretention in the product cyclobutene. In addition, the mechanism must account for the production of the spiro cyclopropane **4** in the reaction of norbornyne with 2,3-dihydropyran.[6] A concerted [2s + 2s] cycloaddition can explain the stereochemistry, though in violation of the rules of conservation of orbital symmetry. We proposed the [2 + 1] pathway outlined in Scheme 2 to account for both the stereochemistry and the spiro product.[6,7] We now address the questions of whether the alternative diradical pathway competes with the concerted pathway and whether it can account for the experimental observations.

Assessing the energetic preference of the two competing pathways is complicated by some disagreements between the computational methods. This needs to be tempered by understanding that B3LYP will tend to favor closed-shell species whereas CASSCF will do the opposite, as noted earlier. The nature of the reaction surface is simply very sensitive to the methodology employed and so we report and discuss a variety of methodologies to try to achieve a consensus conclusion.

In general, the two (U)B3LYP models give similar results, indicating that the size of the basis set is not an

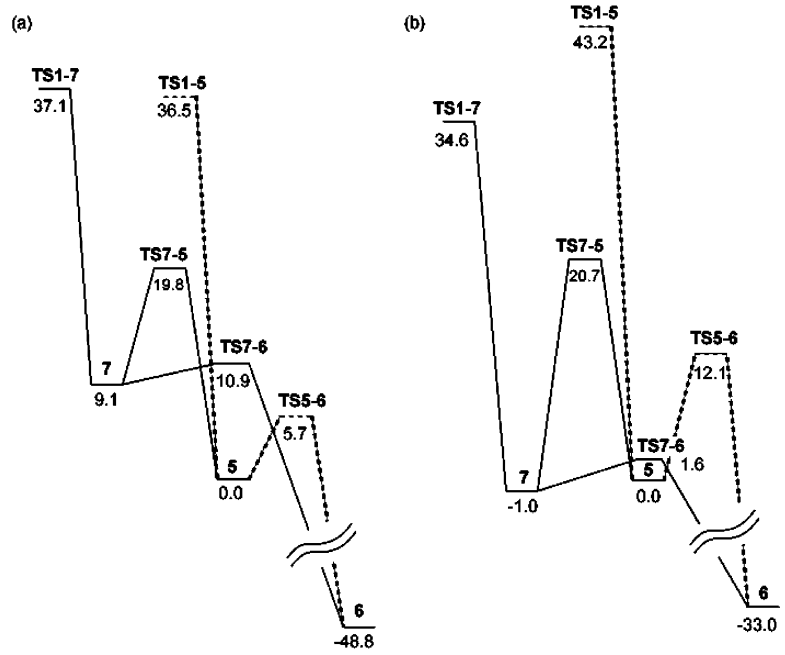

FIGURE 3. Potential energy surfaces for the concerted (dashed line) and stepwise (solid line) reactions of cyclopentyne with ethene. Relative free energies in kcal mol^{-1}: (a) energies at (U)B3LYP/6-31G*; (b) energies at CASSCF(4,4)/6-31G*.

issue. Figure 3a presents a schematic of the potential energy surface. The concerted pathway (indicated by the dashed line) is preferred over the diradical pathway. The highest energy point is **TS1**−**7**, the transition state to form the diradical intermediate. It is about 1.5 kcal mol^{-1} above **TS1**−**5**, the highest energy point along the concerted pathway. In addition, the carbene **5** is 9−10 kcal mol^{-1} more stable than the diradical **7**.

The two CASSCF models also give at least qualitatively similar results, indicating that the size of the active space is not an issue. Figure 3b shows a schematic of the potential energy surface computed at CASSCF(4,4). Here, the diradical pathway is now favored over the concerted one. The highest energy point is **TS1**−**5**, lying nearly 9 kcal mol^{-1} above **TS1**−**7**. The most significant difference between the CASSCF(4,4) and CASSCF(6,6) results is the lack of the [2 + 1] transition state (**TS1**−**5**) on the CASSCF(6,6) surface; only the diradical pathway is observed at CASSCF(6,6). Further, the diradical **7** is more stable than **5**. The MRMP2 computations suggest that the carbene is slightly more stable than the diradical, but increases the preference for the transition state leading to the diradical.

So, how does one reconcile these results? While not without some bias, the MRMP2 method does incorporate the effects of both dynamic and nondynamic correlation to some extent. These computations indicate a diradical pathway, as do the two CASSCF models. The support for the concerted path is only marginal at DFT, with **TS1**−**5** only slightly below **TS1**−**7**. Therefore, we lean toward the diradical pathway as the preferred option for the process.

Although the concerted pathway is entirely consistent with complete stereoretention in the products, partial or total diastereomerization normally results from diradical processes.[24] In fact, the barrier to rotation about the C_6−C_7 bond in **7** is less than 1 kcal mol^{-1} at UB3LYP/6-31G*. One might expect that if the diradical is formed and has any appreciable lifetime, that rotation about the C_6−C_7 bond would lead to loss of stereochemistry. Since the rotational barrier is so much less than the barrier to close to **5**, complete diastereomerization might be expected. Furthermore, the diradical may close directly to **6** and this barrier is not too much higher that the rotational barrier. Again, rotation about the C_6−C_7 bond in **7** might be expected to occur prior to this direct closure, inducing some diastereomerization.

We believe that the diradical pathway is consistent with stereoretention when dynamic effects are considered. Carpenter has effectively argued that such effects can play a critical role in dictating the choice between reaction channels.[25] Basically, dynamic effects take into account momentum along with the potential energy surface; in other words, one must consider the reaction in phase space. When a molecular array crosses over a transition state, or more properly through a bottleneck in phase space, it does so with momentum in that forward direction and will thus tend to continue in that direction unless some barrier intercedes.

For the reaction at hand, one can consider the approach of ethene in a plane approximately perpendicular to cyclopentyne. Crossing through the transition state bottleneck in the neighborhood of **TS1**−**7**, the ethene fragment has forward momentum that continues to propel it toward cyclopentyne, making the C_1−C_6 bond and keeping C_7 positioned essentially perpendicular to the cyclopentyne ring. This momentum will carry C_7

(24) (a) Montgomery, L. K.; Schueller, K.; Bartlett, P. D. *J. Am. Chem. Soc.* **1964**, *86*, 622−628. (b) Bartlett, P. D.; Cohen, G. M.; Elliott, S. P.; Hummel, K.; Minns, R. A.; Sharts, C. M.; Fukunaga, J. Y. *J. Am. Chem. Soc.* **1972**, *94*, 2899−2902. (c) Doering, W. v. E.; Sachdev, K. *J. Am. Chem. Soc.* **1974**, *96*, 1168−1187. (d) Berson, J. A.; Dervan, P. B.; Malherbe, R.; Jenkins, J. A. *J. Am. Chem. Soc.* **1976**, *98*, 5937−5968. (e) Leber, P. A.; Baldwin, J. E. *Acc. Chem. Res.* **2002**, *35*, 279−287. (f) Baldwin, J. E. *Chem. Rev.* **2003**, *103*, 1197−1212.

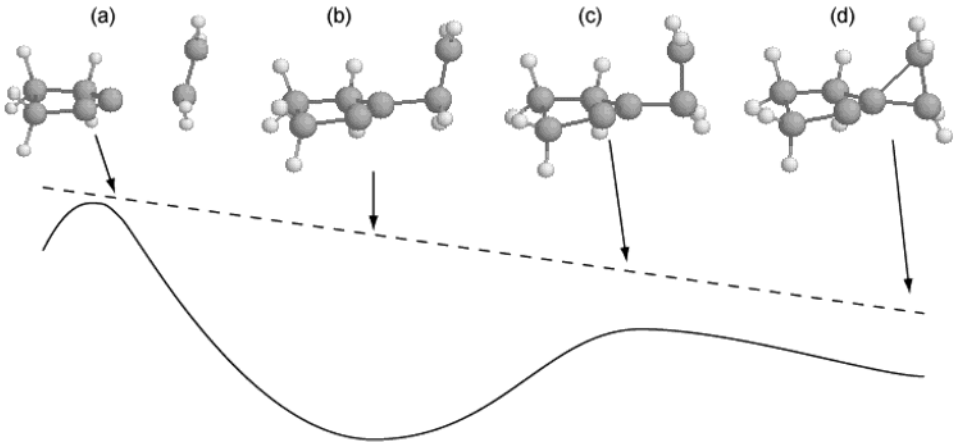

FIGURE 4. Schematic of the trajectory for the reaction following the diradical pathway. The reaction begins by (a) crossing a transition state in the neighborhood of **TS1**−**7** and then (b) passes through the well of the diradical **7**, continuing next to (c) start to form the three-membered ring, and finishing at (d) the carbene **5**. The full line indicates the actual PES, while the dashed line indicates the hypothetical energies of the points along the reaction trajectory.

forward toward C_1 without any twisting about the C_6-C_7 bond. It is this twisting that would lead to diastereomerization, but would involve transfer of momentum from the forward motion into rotational motion, effectively requiring a sharp turn of the complex in phase space. The barrier represented by **TS7**−**5** might aid in deflecting this trajectory and creating rotation about C_6-C_7, but it is much lower in energy than **TS1**−**7**. We expect, therefore, that momentum simply drives the ethene fragment, conformationally unperturbed, forward to culminate in carbene **5**. This process might be pictured in a stylized way as shown in Figure 4. Once **5** is formed, the concerted 1,2-C shift can produce **6** with net overall retention of stereochemistry. The same argument applies to explain the lack of direct closure from the diradical **7** to the product **6**; this route requires transfer of momentum into rotational motion about the C_1-C_6 bond. Another way of framing this argument is that the system passes directly over the potential energy well of the diradical, thereby having essentially no lifetime as the radical. With no residence as the diradical, there is no opportunity for rotation about C_6-C_7 that would lead to diastereomerization. Unfortunately, a molecular dynamics study to test this hypothesis requires computational power that is beyond our current resources. We hope that it will be possible to undertake this study soon, however.

Acknowledgment. The work at The University of Texas at Austin was supported in part by the Robert A. Welch Foundation (Grant F-815).

Supporting Information Available: Coordinates of all structures optimized at (U)B3LYP/6-31G*, (U)B3LYP/6-311+G**, CASSCF(4,4)/6-31G*, and CASSCF(6,6)/6-31G* structures, their absolute energies, and the number of imaginary frequencies. This material is available free of charge via the Internet at http://pubs.acs.org.

JO0492970

(25) (a) Carpenter, B. K. *Acc. Chem. Res.* **1992**, *25*, 520−528. (b) Carpenter, B. K. *Am. Sci.* **1997**, *85*, 138−149. (c) Carpenter, B. K. *Angew. Chem., Int. Ed.* **1998**, *37*, 3341−3350.